Actinide embedded nearly planner gold superatom: structural properties and applications in surface-enhanced Raman scattering (SERS)

Jianpeng Wang,[a,b] Weiyu Xie,[a,b] Jia Wang,[a,b] Yang Gao,[a,b] Jiehong Lei,[*c] Rui-Qin Zhang [*d,e] and Zhigang Wang*[a,b]

a. Institute of Atomic and Molecular Physics, Jilin University, Changchun 130012, China.

b. Jilin Provincial Key Laboratory of Applied Atomic and Molecular Spectroscopy (Jilin University), Changchun 130012, China.

c. Physics and Space Science College, China West Normal University, Nanchong 637009, China

d. Department of Physics, City University of Hong Kong, Hong Kong SAR, P. R. China

e. Beijing Computational Science Research Center, Beijing 100193, China

Part 1: Coordinates of the optimized structures.

Table S1. Coordinates of An@Au_6 (An = Ac^{-1}, Th, Pa^{+1}) and their corresponding adsorption complexes.

Structure	Number	Atom	x (Å)	y (Å)	z (Å)
$[Ac@Au_6]^-$	1	Ac	-0.000001	0.000003	1.162790
	2	Au	0.000021	2.805040	0.101657
	3	Au	2.429440	1.402610	0.102270
	4	Au	2.429360	-1.402540	0.101955
	5	Au	-0.000029	-2.805070	0.101692
	6	Au	-2.429410	-1.402590	0.102223
	7	Au	-2.429380	1.402550	0.102001
Structure	Number	Atom	x (Å)	y (Å)	z (Å)
Th@Au_6	1	Th	0.000000	0.000003	0.687325
	2	Au	-0.000011	2.780150	-0.000116
	3	Au	2.407600	1.390030	-0.000530
	4	Au	2.407670	-1.390100	-0.000072
	5	Au	0.000008	-2.780140	-0.000167
	6	Au	-2.407600	-1.390030	-0.000524
	7	Au	-2.407670	1.390080	-0.000122
Structure	Number	Atom	x (Å)	y (Å)	z (Å)
$[Pa@Au_6]^+$	1	Pa	0.000011	-0.000002	0.002544
	2	Au	0.000055	2.765890	-0.000395
	3	Au	-2.400990	1.385140	-0.000439
	4	Au	-2.400970	-1.385110	-0.000420
	5	Au	2.400940	1.385060	-0.000454
	6	Au	2.400880	-1.385020	-0.000409
	7	Au	0.000062	-2.765960	-0.000428
Structure	Number	Atom	x (Å)	y (Å)	z (Å)
$[Ac@Au_6]^-$+Pyridine	1	Au	1.118850	2.634870	-0.357089
	2	Au	2.752690	0.328769	-0.367115
	3	Au	1.607140	-2.247430	-0.369267

Structure	Number	Atom	x (Å)	y (Å)	z (Å)
	4	Au	-1.681140	2.334290	-0.530085
	5	Au	-1.197730	-2.545680	-0.453127
	6	Au	-2.824770	-0.240494	-0.613826
	7	Ac	-0.084212	0.046006	0.598093
	8	C	-0.078404	1.203100	4.051200
	9	C	-0.130734	1.252480	5.444910
	10	C	-0.386365	-1.093250	4.045790
	11	C	-0.451570	-1.133880	5.438960
	12	C	-0.320967	0.061601	6.149880
	13	N	-0.203319	0.052795	3.360910
	14	H	-0.601338	-2.085730	5.948500
	15	H	0.069028	2.109130	3.458020
	16	H	-0.023871	2.208120	5.958100
	17	H	-0.483007	-2.002390	3.447020
	18	H	-0.366250	0.066063	7.240190

Structure	Number	Atom	x (Å)	y (Å)	z (Å)
Th@Au_6+Pyridine	1	Au	1.106180	2.606990	-0.284348
	2	Au	2.732110	0.327410	-0.267760
	3	Au	1.591270	-2.227100	-0.284178
	4	Au	-1.673730	2.315470	-0.439455
	5	Au	-1.191960	-2.518200	-0.374012
	6	Au	-2.811740	-0.238383	-0.516181
	7	Th	-0.071306	0.045411	0.321450
	8	C	-0.071101	1.211290	3.539240
	9	C	-0.126484	1.253640	4.928800
	10	C	-0.351619	-1.106320	3.532840
	11	C	-0.416898	-1.141960	4.922350
	12	C	-0.302725	0.057621	5.630590
	13	N	-0.181978	0.050649	2.853750
	14	H	-0.554937	-2.094230	5.432780
	15	H	0.065859	2.114630	2.939070
	16	H	-0.033298	2.208130	5.445250

Structure	Number	Atom	x (Å)	y (Å)	z (Å)
	17	H	-0.436397	-2.013170	2.928300
	18	H	-0.350633	0.060654	6.720510

Structure	Number	Atom	x (Å)	y (Å)	z (Å)
$[Pa@Au_6]^+$+Pyridine	1	Au	1.089920	2.564900	-0.289647
	2	Au	2.700650	0.324244	-0.153565
	3	Au	1.570300	-2.198080	-0.219278
	4	Au	-1.657890	2.286600	-0.373395
	5	Au	-1.174930	-2.476160	-0.379239
	6	Au	-2.790400	-0.234649	-0.396285
	7	Pa	-0.062690	0.044914	0.132049
	8	C	-0.071437	1.219680	3.210270
	9	C	-0.128886	1.257270	4.597220
	10	C	-0.328900	-1.115230	3.205370
	11	C	-0.393765	-1.145680	4.592570
	12	C	-0.292398	0.057509	5.298890
	13	N	-0.170169	0.049995	2.525490
	14	H	-0.521633	-2.098650	5.104190
	15	H	0.056657	2.124320	2.610770
	16	H	-0.046283	2.212810	5.113260
	17	H	-0.404461	-2.023740	2.602760
	18	H	-0.339816	0.062664	6.388400

Part 2. Calculated relative energies for An@Au_6 (An = Ac^-, Th, Pa^+).

Table S2. Relative bonding energies for An@Au_6 calculated based on different functionals and basis sets.

System	Functional /Basis set	Multiplicity	ΔE (eV)
$[Ac@Au_6]^-$	BP86/TZP	1(C_{6v})	0
		3(C_{6v})	1.54
		5(C_{3v})	2.7
	PBE/TZP	1(C_{6v})	0
		3(C_{6v})	1.56
		5(C_{3v})	2.68
Th@Au_6	BP86/TZP	1(C_{6v})	0
		3(C_{6v})	1.59
		5(C_{3v})	2.97
	PBE/TZP	1(C_{6v})	0
		3(C_{6v})	1.61
		5(C_{3v})	2.95
$[Pa@Au_6]^-$	BP86/TZP	1(D_{6h})	0
		3(C_{6v})	0.18
		5(C_{3v})	1.18
	PBE/TZP	1(D_{6h})	0
		3(C_{6v})	0.22
		5(C_{3v})	1.38

Part 3. Calculated geometry information of An@Au_6.

Table S3. Symmetry, gold-gold bond (nm), metal-gold bond (nm), gold-metal-gold angle (°), HOMO-LUMO gap (eV), bond energy (eV) of $[Ac@Au_6]^-$, Th@Au_6 and $[Pa@Au_6]^+$, respectively.

	$[Ac@Au_6]^-$	Th@Au_6	$[Pa@Au_6]^+$
Symmetry	C_{6v}	C_{6v}	D_{6h}
Au-Au (Å)	2.81 (2.79)	2.78 (2.77)	2.77 (2.76)
An-Au (Å)	3.00 (3.01)	2.86 (2.87)	2.77 (2.76)
Au-An-Au angle (°)	138.8 (136.5)	152.1 (151.5)	180.0 (180.0)
HOMO-LUMO Gap (eV)	1.98 (1.91)	1.80 (1.70)	0.15 (0.0)
Bond Energy (eV)	-21.36 (-48.41)	-21.00 (-49.15)	-13.91 (-42.69)

The data in parenthesis were obtained with SOC (spin-orbit coupling) effects included.

Part 4. Charge analysis for An@Au$_6$.

Table S4. Hirshfeld Charge Analysis and VDD analysis.

Atom	Hirshfeld (e)	VDD (e)
Th	0.4066	0.538
Au	-0.0678	-0.09
Au	-0.0678	-0.09
Au	-0.0678	-0.09
Au	-0.0678	-0.09
Au	-0.0678	-0.09
Au	-0.0678	-0.09
Ac	0.3168	0.458
Au	-0.2195	-0.243
Au	-0.2195	-0.243
Au	-0.2195	-0.243
Au	-0.2195	-0.243
Au	-0.2195	-0.243
Au	-0.2195	-0.243
Pa	0.5943	0.684
Au	0.0676	0.053
Au	0.0676	0.053
Au	0.0676	0.053
Au	0.0676	0.053
Au	0.0676	0.053
Au	0.0676	0.053

Part 5. The vibrational modes and the vibrational spectra for An clusters

To facilitate future experimental characterizations, we also computed the vibrational spectra of An@Au_6 (An = Ac^-, Th, Pa^+). The results show that breathing vibration mode at 120 cm^{-1}, 131 cm^{-1} and 132 cm^{-1} for $[Ac@Au_6]^-$, Th@Au_6 and $[Pa@Au_6]^+$ are Raman-active but IR-inactive. But actinide translation vibration mode at 133 cm^{-1},157 cm^{-1} and 176 cm^{-1} for $[Ac@Au_6]^-$, Th@Au_6 and $[Pa@Au_6]^+$ are IR-active but Raman-inactive.

Figure 1. IR and Raman vibration modes of An@Au_6 (An = Ac^-, Th, Pa^+) clusters.

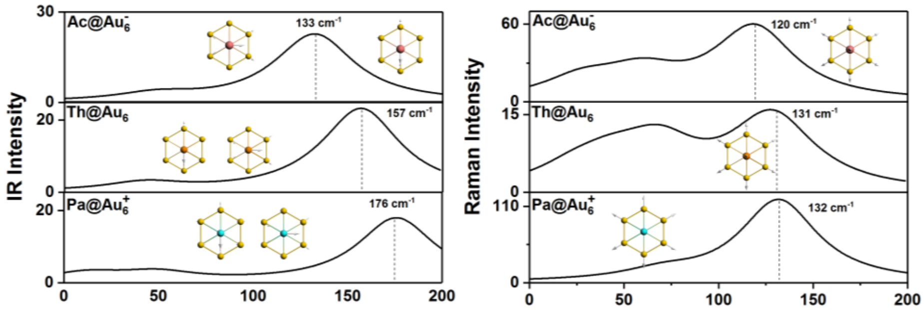

Part 6. Energy decomposition analysis for An@Au_6.

Table S5. Bond energy decomposition (eV).

Bond energy decomposition (eV)			
	$[Ac@Au_6]^-$ (Case 6)	Th@Au_6 (Case 2)	$[Pa@Au_6]^+$ (Case 10)
$\triangle E_{int}$	-11.7045	-10.8909	-3.4128
$\triangle E_{pauli}$	32.7356	53.5959	48.5546
$\triangle E_{orb}$	-20.0051	-33.4525	-16.7198
	45.02%	51.87%	32.17%
$\triangle E_{elestat}$	-24.4349	-31.0343	-35.2476
	54.98%	48.13%	67.83%
	Ac@Au_6 (Case 7)	Th@Au_6 (Case 2)	Pa@Au_6 (Case 11)
$\triangle E_{int}$	-8.3811	-10.8909	-10.109
$\triangle E_{pauli}$	32.7356	53.5959	48.5546
$\triangle E_{orb}$	-16.6818	-33.4525	-23.416
	40.57%	51.87%	39.92%
$\triangle E_{elestat}$	-24.4349	-31.0343	-35.2476
	59.43%	48.13%	60.08%

Table S6. The various cases for fragment electron configurations assumed for EDA.

#Default closed shell singlet state for each fragment. Au6* is the ground state for Au6 ring.

	$\triangle$E in eV	$\triangle E_{int}$	$\triangle E_{Pauli}$	$\triangle E_{ele}$	$\triangle E_{orb}$ (percentage of total attractive)
Case 1	#	-12.09	59.01	-29.99	-41.11 (57.82%)
Case 2	**Th↑↑+Au_6^***	**-10.89**	**53.6**	**-31.03**	**-33.45 (51.87%)**
Case 3	Th↑↑↑↑+Au_6↓↓↓↓	-14.56	28.26	-25.02	-17.8 (41.56%)
Case 4	Th↑↑+Au_6↓↓↓↓	-12.95	41.41	-30.72	-23.64 (43.49%)
Case 5	$[\#]^{-1}$	-11.81	44.36	-24.43	-31.74 (56.50%)
Case 6	**$[Ac\uparrow+Au_6^*]^{-1}$**	**-11.7**	**32.74**	**-24.43**	**-20.01 (45.02%)**
Case 7	**$[Ac\uparrow+Au_6^*]$**	**-8.38**	**32.74**	**-24.43**	**-16.68 (40.57%)**
Case 8	Ac↑↑↑↑+Au_6↓↓↓↓	-16.38	28.29	-28.5	-16.17 (36.21%)

Case 9	$[\#]^{+1}$	-5.23	49.36	-32.69	-21.89 40.11% ()
Case 10	**$[Pa7s{\uparrow}{\downarrow}6d{\uparrow}5f{\uparrow}{\uparrow}+Au_6^{*}]^{+1}$**	**-3.41**	**48.55**	**-35.25**	**-16.72 (32.17%)**
Case 11	**$[Pa7s{\uparrow}{\downarrow}6d{\uparrow}5f{\uparrow}{\uparrow}+Au_6^{*}]$**	**-10.11**	**48.55**	**-35.25**	**-23.42 39.92% ()**
Case 12	$[Pa6d{\uparrow}{\uparrow}{\uparrow}{\uparrow}+Au_6{\downarrow}{\downarrow}{\downarrow}{\downarrow}]^{+1}$	-15.8	29.17	-20.04	-24.93 (55.45%)
Case 13	$[Pa6d{\uparrow}{\uparrow}{\uparrow}{\uparrow}+Au_6^{*}]^{+1}$	-13.74	27.62	-20.6	-20.76 (50.18%)
Case 14	$[Pa7s{\uparrow}{\downarrow}5f{\uparrow}{\downarrow}+Au_6^{*}]^{+1}$	-9.81	40.87	-26.3	-24.37 (48.09%)

Total interaction can be decomposed as:

$$\triangle E_{int} = \triangle E_{elestat} + \triangle E_{Pauli} + \triangle E_{orbital}$$

where $\triangle E_{elestat}$ is the electrostatic interaction term; $\triangle E_{Pauli}$ is the Pauli repulsion term; $\triangle E_{orbital}$ is the orbitals interaction term. Within this energy decomposition scheme the attractive and repulsive terms are negative and positive, respectively.

Part 7. UV–visible absorption spectra.

The absorption spectrum can be an effective identification method to test the validity of the specific superatom, especially in the low-energy range The allowed transitions involve mainly the SAMOs.[1-3] The first peak near 435 nm originates from 1P to 1D transition. The next peak near 462 nm arises from the 1D to 1F transition. And the weak peak around 518 nm arises from 1D to (1F, 5f) transition. The last peak around 571 nm arises from 1D to 1D transition. For $[Ac@Au_6]^-$ clusters, the weak peak at 383 nm arises from 1P to 1D transition. The next peak around 412 nm originates from 1P to orbital dominated by 7s of Ac. Strong peak near 465 nm arises from 1D to 1F transition and the last one at 498 arises from 1D to 1D transition. Inclusion of SOC effects causes all peaks shifting to red.

Table S7. Calculated wavelength (λ in nm), oscillator strength, and weights of $Th@Au_6$ and $[Ac@Au_6]^-$ clusters at BP86/TZP including scalar relativistic effects.

	state	λ	f	transition		weight
	$5E_1$	435	0.0134	$1P_x$ $1P_y$	$1D_{z^2}$	0.9230
	$4E_1$	462	0.0700	$1D_{xy}$ $1D_{x^2-y^2}$	$1F_x$	0.4602
				$1D_{xy}$ $1D_{x^2-y^2}$	$1F_y$	0.3417
$Th@Au_6$	$1A_1$	516	0.0022	$1D_{xy}$ $1D_{x^2-y^2}$	5f [Th 91.37%]	0.9947
	$3E_1$	523	0.0013	$1D_{xy}$ $1D_{x^2-y^2}$	$1F_y$	0.4982
				$1D_{xy}$ $1D_{x^2-y^2}$	$1F_x$	0.4659
	$1E_1$	571	0.0147	$1D_{xy}$ $1D_{x^2-y^2}$	$1D_{xz}$ $1D_{yz}$	0.9651
	$1A_1$	357	0.0200	$1P_x$ $1P_y$	$1D_{xz}$ $1D_{yz}$	0.9244
	$4E_1$	383	0.0048	$1P_x$ $1P_y$	$1D_{z^2}$	0.9773
$[Ac@Au_6]^-$	$3E_1$	412	0.0609	$1P_x$ $1P_y$	7s [Ac 79.60%]	0.9237
	$2E_1$	465	0.1930	$1D_{xy}$ $1D_{x^2-y^2}$	$1F_y$	0.8547
	$1E_1$	498	0.0226	$1D_{xy}$ $1D_{x^2-y^2}$	$1D_{xz}$ $1D_{yz}$	0.9663

Note: $Th@Au_6$: P_x [Au 6s 46.28%, 5d 42.76%; Th 7p 4.47%]; P_y [Au 6s 46.28%, 5d 42.76%; Th 7p 4.47%]; D_{xy} [Au 7s 49.39%, 5d 21.30%, 6p 13.61%; Th 6d 13.63%]; $D_{x^2-y^2}$ [Au 7s 49.39%, 5d 21.30%, 6p 13.61%; Th 6d 13.63%]; D_{z^2} [Th 6d 63.99%, 7s 19.59%, 5f 5.52%; Au 5d 4.68%]; F_x [Th 5f 79.60%; Au 6p 14.80%, 5d 4.82%]; F_y [Au 6s 45.00%, 5d 13.87%; Th 5f 41.45%];

$[Ac@Au_6]^-$: P_x [Au 5d 51.09%, 6s 40.87%; Ac 7p 1.79%]; P_y [Au 5d 51.09%, 6s 40.87%; Ac 7p 1.79%]; D_{xy} [Au 6s 58.13%, 6p 12.86%, 5d 16.39%; Ac 6d 11.27%]; $D_{x^2y^2}$ [Au 6s 58.13%, 6p 12.86%, 5d 16.39%; Ac 6d 11.27%]; D_{xz} [Ac 6d 68.66%; Au 6p 10.97%, 7s 7.37%]; D_{yz} [Ac 6d 68.66%; Au 6p 10.97%, 7s 7.37%]; D_{z^2} [Ac 6d 62.38%; Au 6p 23.06%]; F_y [Au 6s 98.29%; Ac 5f 1.93%].

References

1. Y. Negishi, K. Nobusada and T. Tsukuda, *Journal of the American Chemical Society*, 2005, **127**, 5261-5270.
2. C. M. Aikens, *The Journal of Physical Chemistry Letters*, 2011, **2**, 99-104.
3. O. Lopez-Acevedo, H. Tsunoyama, T. Tsukuda, H. Häkkinen and C. M. Aikens, *Journal of the American Chemical Society*, 2010, **132**, 8210-8218.